

Targeted Assessment of Mucosal Immune Gene Expression Predicts Clinical Outcomes in Children with Ulcerative Colitis

Kathryn Clarkston,^{a,d}  Rebekah Karns,^a Anil G. Jegga,^{b,c} Mihika Sharma,^b Sejal Fox,^a Babajide A. Ojo,^e Phillip Minar,^{a,c} Thomas D. Walters,^f  Anne M. Griffiths,^f David R. Mack,^g Brendan Boyle,^h Neal S. LeLeiko,ⁱ James Markowitz,^j Joel R. Rosh,^k Ashish S. Patel,^l Sapana Shah,^m Robert N. Baldassano,ⁿ Marian Pfefferkorn,^o Cary Sauer,^p Subra Kugathasan,^p  Yael Haberman,^{a,c,q} Jeffrey S. Hyams,^r Lee A. Denson,^{a,c}  Michael J. Rosen^{e,a,c} 

^aDivision of Gastroenterology, Hepatology and Nutrition,

^bDivision of Biomedical Informatics, Cincinnati Children's Hospital Medical Center, Cincinnati, OH, USA

^cDepartment of Pediatrics, University of Cincinnati College of Medicine, Cincinnati, OH, USA

^dDivision of Pediatric Gastroenterology, Children's Mercy Hospital, University of Missouri-Kansas City School of Medicine, Kansas City, MO, USA

^eDivision of Pediatric Gastroenterology, Department of Pediatrics, Stanford University School of Medicine, Stanford, CA, USA

^fDivision of Pediatric Gastroenterology, Hospital for Sick Children, Toronto, ON, Canada,

^gDivision of Gastroenterology, Hepatology and Nutrition, Children's Hospital of Eastern Ontario and University of Ottawa, Ottawa, ON, Canada,

^hDivision of Gastroenterology, Hepatology, and Nutrition, Nationwide Children's Hospital, Columbus, OH, USA

ⁱDepartment of Pediatrics, Columbia University Vagelos College of Physicians and Surgeons and NewYork-Presbyterian Morgan Stanley Children's Hospital, New York, NY, USA

^jDivision of Gastroenterology, Hepatology, and Nutrition, Cohen Children's Medical Center of New York, New Hyde Park, NY, USA

^kDivision of Gastroenterology, Hepatology, and Nutrition, Goryeb Children's Hospital, Atlantic Health, Morristown, NJ, USA

^lDivision of Gastroenterology, Phoenix Children's Hospital, Phoenix, AZ, USA

^mDivision of Gastroenterology, Hepatology and Nutrition, UPMC Children's Hospital of Pittsburgh, Pittsburgh, PA, USA

ⁿDivision of Gastroenterology, Hepatology and Nutrition, Children's Hospital of Philadelphia, Philadelphia, PA, USA

^oDivision of Gastroenterology, Hepatology, and Nutrition, Riley Children's Hospital, Indianapolis, IN, USA

^pDivision of Gastroenterology, Hepatology and Nutrition, Department of Pediatrics, Emory University and Children's Healthcare of Atlanta, Atlanta, GA, USA

^qSheba Medical Center, Tel Hashomer, Israel,

^rDivision of Digestive Diseases, Hepatology, and Nutrition, Connecticut Children's Medical Center, Hartford, CT, USA

Corresponding author: Michael J. Rosen, MD, MSCI, Division of Pediatric Gastroenterology, Department of Pediatrics, Stanford University School of Medicine, 750 Welch Rd, Suite 116, Palo Alto, CA 94304, USA. E-mail: rosenm@stanford.edu

Abstract

Background and Aims: We aimed to determine whether a targeted gene expression panel could predict clinical outcomes in paediatric ulcerative colitis [UC] and investigated putative pathogenic roles of predictive genes.

Methods: In total, 313 rectal RNA samples from a cohort of newly diagnosed paediatric UC patients (PROTECT) were analysed by a real-time PCR microfluidic array for expression of type 1, 2 and 17 inflammation genes. Associations between expression and clinical outcomes were assessed by logistic regression. Identified prognostic markers were further analysed using existing RNA sequencing (RNA-seq) data sets and tissue immunostaining.

Results: *IL13RA2* was associated with a lower likelihood of corticosteroid-free remission (CSFR) on mesalamine at week 52 ($p = .002$). A model including *IL13RA2* and only baseline clinical parameters was as accurate as an established clinical model, which requires week 4 remission status. *RORC* was associated with a lower likelihood of colectomy by week 52. A model including *RORC* and PUCAL predicted colectomy by 52 weeks (area under the receiver operating characteristic curve 0.71). Bulk RNA-seq identified *IL13RA2* and *RORC* as hub genes within UC outcome-associated expression networks related to extracellular matrix and innate immune response, and lipid metabolism and microvillus assembly, respectively. Adult UC single-cell RNA-seq data revealed *IL13RA2* and *RORC* co-expressed genes were localized to inflammatory fibroblasts and undifferentiated epithelial cells, respectively, which was supported by protein immunostaining.

Conclusion: Targeted assessment of rectal mucosal immune gene expression predicts 52-week CSFR in treatment-naïve paediatric UC patients. Further exploration of *IL13RA2* as a therapeutic target in UC and future studies of the epithelial-specific role of *RORC* in UC pathogenesis are warranted.

Key Words: Paediatric inflammatory bowel disease; gene expression array; weighted gene co-expression network analysis

1. Introduction

The prevalence of ulcerative colitis [UC] in children is rising worldwide.^{1–4} Children with UC are initially treated with mesalamine or corticosteroids [CS] based on disease severity and therapy is escalated when corticosteroid-free remission [CSFR] is not achieved. Unsuccessful therapeutic trials expose patients to adverse drug effects and delay sustained remission. There is a need for predictors of treatment response that inform individualized treatment plans and target the safest and most effective medication to each unique patient.

Predicting Response to Standardized Pediatric Colitis Therapy [PROTECT] was a prospective clinical trial of standardized treatment with mesalamine with or without corticosteroids [based on disease severity] in paediatric patients newly diagnosed with UC. PROTECT demonstrated that 38% achieve CSFR at 1 year on mesalamine alone, but the remainder require a progression to thiopurines [19%], anti-tumour necrosis factor [TNF] biological agents [31%] or colectomy [6%.⁵ PROTECT produced a clinical predictive model for CSFR on mesalamine at 52 weeks that included baseline Pediatric Ulcerative Colitis Activity Index [PUCAI] score, haemoglobin and clinical remission at week 4. Notably, this predictive model relies on week 4 clinical status, and an opportunity exists to develop models from baseline clinical and molecular data alone.

Type 2 inflammation is defined by the production of interleukin [IL]-4, IL-5 and IL-13 cytokines by T helper 2 cells and group 2 innate lymphoid cells, which are involved in helminth eradication and allergic disease.⁶ Early studies of the mucosal immune response in human inflammatory bowel disease [IBD] identified an atypical type 2 immune response in adult UC, which was proposed to be pathogenic.⁷ However, collective evidence supports a mixed immune response in UC that also includes type 1 and type 17 inflammation, and the precise role of type 2 inflammation remains unclear.⁶ We previously showed that mucosal expression of type 2 and type 17 immune response genes, as assessed by a real-time reverse-transcription quantitative polymerase chain reaction [RT-qPCR] microfluidic array, distinguishes children with treatment-naïve UC from colonic Crohn's disease, and that a type 2 immune gene expression profile characterized by detectable *IL13* expression was associated with favourable treatment response in paediatric UC.⁸ However, this study was limited by the small cohort of UC patients studied and treatment heterogeneity.

The aim of the present study was to evaluate the prognostic ability of our RT-qPCR microfluidic array, focusing on type 1, 2 and 17 immune response genes as previously described,⁸ for predicting clinical outcomes in a larger paediatric UC cohort on standardized therapy. We opted to use a RT-qPCR array because of our prior smaller study indicating prognostic value,⁸ the high sensitivity of RT-qPCR for detecting gene expression, the targeted approach does not require as severe a multiple comparison statistical penalty compared to genome-wide expression approaches, and multiple RT-qPCR gene expression assays have been advanced to clinical use for informing cancer treatment.⁹ Identified prognostic gene expression markers were further studied using existing bulk and single-cell colon tissue RNA sequencing [RNA-seq] data and tissue immunostaining to identify their cellular sources and propose putative roles in disease pathogenesis.

2. Materials and Methods

2.1. PROTECT cohort rectal RNA samples

Rectal mucosal RNA, clinical and histopathologic data were obtained from the PROTECT study, a 29-centre cohort of 428 patients aged 4–17 years with a new diagnosis of UC initially treated with mesalamine with or without CS induction therapy and followed for 52 weeks.⁵ Eligibility criteria, key dates, study size and blinding approaches were previously published.^{5,10} Baseline rectal biopsies were obtained in 367 [85%] of PROTECT cohort patients and were processed for RNA and DNA isolation. A follow-up research endoscopy with biopsies at 52 weeks for assessment of endoscopic healing was obtained in 98 [23%] patients. Centralized Mayo Endoscopic scoring and histopathological assessment were performed at baseline and 52 weeks. We assayed high-integrity RNA from 313 baseline and 58 follow-up PROTECT samples. Biopsies from 20 patients without IBD and with normal rectal histopathology enrolled under a separate institutional review board [IRB]-approved protocol at Cincinnati Children's Hospital Medical Center were included for analysis as controls.¹¹

2.2. Ethical approval

The PROTECT study [ClinicalTrials.gov NCT 01536535] was approved by each centre's IRB, and each participant provided informed consent or assent as applicable. Rectal mucosal biopsy tissue samples from paediatric UC and non-IBD patients used for immunostaining were collected under an IRB-approved protocol at Cincinnati Children's Hospital Medical Center.

2.3. Real-time RT-qPCR

Rectal RNA was analysed by custom microfluidic RT-qPCR gene expression array [GEA] for expression of 24 genes related to type 1, type 2, type 17 and regulatory immune responses as previously described.⁸ In total, 200 ng of rectal RNA from diagnostic and week 52 follow-up endoscopies of PROTECT participants was analysed. RNA quality control was performed on 100 ng RNA from each PROTECT sample using an Agilent 2100 Bioanalyzer in the CCHMC Digestive Health Center. Only samples with an RNA integrity number [RIN] ≥ 7 were used. cDNA was synthesized from the rectal RNA samples, then RT-qPCRs were performed on custom TaqMan array 384-well microfluidic cards [ThermoFisher] and run on a 7900HT Fast Real-Time PCR System in the CCHMC Division of Gastroenterology. Twenty-four distinct gene expression assays related to type 1, type 2, type 17 and regulatory immune responses [Supplementary Table 1] were performed in duplicate. GAPDH was previously validated as the reference gene with the least variability between IBD and control patients, and expression relative to non-IBD controls was calculated using a modification of the $2^{-\Delta\Delta C_q}$ method previously described.⁸

2.4. Outcomes

The primary outcome was the association of baseline gene expression with CSFR on mesalamine at 52 weeks, which was the PROTECT primary endpoint.⁵ CSFR was defined as PUCAI score < 10 , no corticosteroids within 28 days of assessment, and no additional medical therapy or colectomy. Secondary outcomes included corticosteroid-naïve [never required CS] remission on mesalamine therapy [CSNR] at

12 and 52 weeks, escalation to infliximab [IFX] in patients with baseline moderate-to-severe disease [defined by the PROTECT study as initial treatment with oral CS and baseline PUCAI ≥ 45 or IV CS] by 52 weeks, colectomy in the baseline moderate-to-severe disease group by 52 weeks, CSFR on IFX in those who escalated to IFX therapy by 12 weeks and endoscopic healing [endoscopic Mayo score = 0] at 52 weeks.

2.5. Statistical analysis

SAS version 9.4 was used to conduct statistical analyses. Baseline characteristics of subgroup populations were compared using the chi-square test for categorical variables and Wilcoxon's rank-sum non-parametric test for continuous variables. Differences in gene expression in UC patients compared to controls was assessed using a Wilcoxon rank-sum non-parametric test with false discovery rate correction for multiple comparisons. Unsupervised hierarchical clustering was used to identify patient clusters with unique gene expression patterns and Fisher's exact test was used to assess associations between analyte clusters and outcomes. Correlations between mucosal gene expression and baseline mucosal eosinophil count and endoscopic scores were assessed by Spearman's correlation coefficient. To mirror the PROTECT study analysis,⁵ univariable and multivariable logistic regression analyses were performed excluding a small subset of patients with protocol violations, with a final $n = 284$ for our GEA analysis. Univariable logistic regression was performed to assess the association of analytes and clinical variables against each outcome. Associations with a p -value < 0.1 were entered into multivariable analysis. When expression values of multiple genes were highly correlated, only the gene with the strongest significance was included in multivariable analysis. Results from multivariable analyses were integrated into existing PROTECT models or incorporated with clinical and histopathological data to develop new predictive models. Samples with missing data were excluded only from analyses that involved the variables for which they had missing information. Results were assessed with receiver operating characteristic [ROC] curves and corresponding area under the curve [AUC], sensitivity, specificity, positive predictive value [PPV] and negative predictive value [NPV]. We used a probability of 0.5 to set cut-off points for predictive performance characteristics for all outcomes except colectomy. A probability of 0.2 was used for colectomy, given the low incidence of colectomy at 52 weeks in this cohort. Differences in model performance were assessed using the likelihood ratio test. Complete univariable logistic regression associations are listed in [Supplementary Table 4](#).

2.6. Weighted gene co-expression network analysis

Weighted gene co-expression network analysis [WGCNA] was applied as previously described^{12,13} to available PROTECT study RNA-seq data, to generate co-expression modules for outcome correlation and downstream network and functional annotation analyses. An adjacency matrix was constructed using a power value of 5 for soft thresholding. Co-expressed gene modules were dynamically identified with module size set to 30 and *deepSplit* to 4 to control the sensitivity for cluster splitting. Gene expression profiles within each module were represented by the first principal component, or eigengene, and correlated with phenotypic traits to identify candidate modules.¹³ Modules with similar expression

profiles were merged and the eigengenes were clustered using the 'average' method with threshold set to 0.1. Both connectivity- and phenotype-based significance scores were used to identify hub genes within candidate modules, as previously described, and the Pearson correlation coefficient was calculated.¹² Functional enrichment analysis was performed using the ToppFun application of the ToppGene Suite,¹⁴ with the top 200 correlated genes to *IL13RA2* and *RORC* from their respective black and brown modules as the input gene sets. Functional enrichment network visualizations for the *IL13RA2* and *RORC* gene sets were generated utilizing the top ten enriched terms and the Cytoscape application.¹⁵

2.7. Single-cell RNA-seq analysis

We analysed a publicly available adult human colon UC single-cell data set to examine cell-specific expression of gene co-expression modules of interest.¹⁶ Genes of interest along with their 20 most highly correlated genes within modules identified by WGCNA were assessed for cell-specific expression amongst subsets of colon epithelial, immune and stromal cells to assess the probable cellular source of each co-expression module. To further determine what cells were driving disease-associated differential expression of genes of interest, normalized cell-specific expression in cells expressing those genes were compared between disease states using the Kruskal–Wallis test with Dunn's post-test for multiple comparisons.

2.8. *IL13-Ra2* and *RORγ* immunostaining

For immunofluorescence analysis, formalin-fixed paraffin-embedded inflamed rectum, sigmoid or descending colon tissue sections from ten PROTECT patients and histologically normal tissue sections from eight non-IBD controls were deparaffinized and rehydrated. Antigen retrieval was performed using Tris-based antigen unmasking solution [Vector Laboratories] for 10 min in a pressure cooker. Sections were blocked with 5% donkey serum for 2 h at room temperature and then incubated with primary antibody mouse anti-IL13-Ra2 [Abcam, ab55275] and rabbit anti-CD3 [Abcam, ab135372] or rabbit anti-vimentin [Abcam, ab92547] in 5% donkey serum overnight at 4°C. Sections were washed with 0.1% BSA and 0.05% Tween/PBS and incubated with donkey anti-mouse Alexa Fluor 488 and donkey anti-rabbit Alexa Fluor 647 [Invitrogen] for 2 h at room temperature. Slides were washed in PBS and counterstained with DAPI/Supermount G solution [Southern Biotechnology Associates]. Images were acquired using an Olympus BX51 microscope with a DP80 camera [Olympus America] and CellSens Dimension digital imaging software [Olympus Corporation, version 1.18]. Images were merged using ImageJ 1.52q [FIJI] software [NIH, <https://imagej.nih.gov/ij/>]. Cells co-expressing *IL13-Ra2* and vimentin or CD3 were counted on at least five high-power fields [40× magnification] per patient.

For *RORγ* immunohistochemistry, paraffin-embedded rectal mucosal tissue sections from five UC patients with active endoscopic activity [endoscopic Mayo score 2–3] and histologically normal tissue sections from five non-IBD controls were deparaffinized and rehydrated. Antigen was retrieved at high pressure for 12 min in 10 mM sodium citrate buffer plus 0.05% Tween-20 [pH 6] using a pressure cooker [Bio SB]. The sections were blocked in 10% normal rabbit serum and 1% BSA and incubated with *RORγ* antibody

[Thermo Fisher Scientific, 14-6988-82] for 75 min at room temperature. Endogenous peroxidase activity was quenched with Bloxall [Vector Labs] and incubated with a biotinylated rabbit anti-rat IgG secondary antibody for 60 min at room temperature [Vectastain, BA-4000]. Signals were amplified with the Avidin-Biotin Complex [ABC] Kit [Vector Labs] and ROR γ was detected using 3,3'-diaminobenzidine [DAB, Vector Labs]. The nuclei were counterstained with haematoxylin. Similarly stained serial sections from the same tissues lacking only the primary antibody served as the negative control for each sample. Images of five fields per sample were acquired [20 \times and 60 \times objectives] using a Keyence BZ-X800 inverted microscope for further analyses.

Quantitative analysis of ROR γ in epithelial cells was carried out using ImageJ Fiji software as previously described with modifications.¹⁷ Briefly, the contribution of DAB and haematoxylin staining was calculated and digitally separated with the colour deconvolution plugin.¹⁸ Each deconvoluted image with DAB staining was adjusted to lower and upper thresholds set at 0 and 122, respectively. The freehand tool was used to select the epithelium as the region for analysis. The expression level of ROR γ in the epithelium was estimated by measuring the percentage area fraction with DAB staining. In the lamina propria, ROR γ + cells were manually counted in five high-power field images per section.

3. Results

3.1. Altered rectal mucosal gene expression in UC

Baseline characteristics of the UC and non-IBD participants and the relevant treatment or disease severity subgroups are listed and compared with those of the entire PROTECT cohort in Table 1. Importantly, the PROTECT patients with rectal RNA in this study were similar to the overall PROTECT cohort.

Compared to non-IBD controls, UC patients showed significantly altered rectal expression of all but two studied transcripts: *IL1RL1[m]*, which encodes the membrane-bound IL-33 receptor, and *AREG*, which encodes the type 2 immune response growth factor amphiregulin¹⁹ [Figure 1A]. Most genes were upregulated in the inflamed UC rectum except for *RORC* [which encodes the nuclear receptor ROR γ and its isoform ROR γ t, the canonical Th17 transcription factor], which was downregulated compared to controls.

We previously observed that hierarchical clustering of patients based on expression of 15 genes differentially expressed between UC, non-IBD and Crohn's colitis identified a cluster of patients with higher likelihood of clinical remission. This cluster was primarily defined by detectable *IL13* expression.⁸ Application of the same analysis using these 15 genes did not reveal clearly defined subclusters, and outcomes were not different between clusters [Supplementary Table 3, Supplementary Figure 1]. Therefore, we assessed expression of individual genes for association with treatment-specific outcomes.

3.2. *IL13RA2* expression predicts corticosteroid-free remission on mesalamine at week 52 [CSFR]

In total, 36% of patients with high-quality RNA available achieved CSFR at week 52 on mesalamine alone, which is comparable to the proportion in the overall PROTECT cohort [38%]. Univariable logistic regression revealed that increased expression of *IL13RA2* and *S100A8* were associated with alower likelihood of achieving CSFR [Table 2

and Supplementary Table 4]. There was a trend toward an association of reduced *RORC* expression with lower likelihood of CSFR. *IL13RA2* encodes a decoy receptor for the type 2 cytokine IL-13 that reduces its bioactivity,²⁰ and *S100A8* encodes a subunit of calprotectin. Since *IL13RA2* and *S100A8* expression were highly correlated, we assessed whether *IL13RA2* expression alone improved the PROTECT published model for CSFR. Incorporating *IL13RA2* modestly increased the area under the curve [AUC, from 0.72 to 0.74, $p = .052$] for the published PROTECT model [Table 2]. The existing model includes week 4 remission as a variable, which only allows use of the model after 4 weeks of observation. We found that a baseline data-only model including rectal *IL13RA2* expression, haemoglobin, vitamin D and PUCAI exhibited similar performance [AUC = 0.70] to the published PROTECT model, which includes week 4 remission status [Table 2]. Furthermore, inclusion of *IL13RA2* expression in this baseline model exhibited superior predictive value over a model of haemoglobin, vitamin D and PUCAI alone [$p = .029$]. Of note, baseline faecal calprotectin, a standard measure of mucosal disease severity used in clinical practice, did not predict CSFR by univariable analysis. Furthermore, although histological severity as measured by the Nancy histology index was associated with CSFR by univariable analysis [Supplementary Table 4], it did not add predictive value to the multivariable model. Therefore, *IL13RA2* expression provides more prognostic information than these measures of mucosal disease severity.

3.3. *IL13* expression predicts corticosteroid-naïve remission at week 12 [CSNR]

In total, 48% and 41% of patients who started on mesalamine alone achieved CSNR at week 12 and week 52, respectively. Univariable logistic regression revealed that increased expression of *IL13*, which encodes a type 2 effector cytokine, was significantly associated with the likelihood of achieving CSNR at week 12 [Table 2]. We did not detect any association between expression of genes on the panel and CSNR at week 52.

3.4. *IL13RA2* and *IL33* expression predict escalation to IFX by week 52

In total, 73 [43%] of the 169 patients with baseline moderate-to-severe disease were escalated to IFX by week 52. Univariable logistic regression revealed that increased expression of *IL13RA2* and *IL25*, and decreased expression of *ALOX15* and *IL33*, were associated with the likelihood of escalating to IFX [Table 2]. Multivariable logistic regression revealed that expression of *IL13RA2* and *IL33* [type 2 instructive cytokine] were independently associated with escalation to IFX and predicted this outcome with an AUC of 0.66. The published PROTECT model for escalation to IFX was validated in this subset of patients, but the addition of *IL13RA2* or *IL33* gene expression did not improve model performance.

3.5. No detected gene expression predictors of response to early IFX therapy

Forty-one patients received early treatment with IFX within 12 weeks of diagnosis, and 12 [29%] achieved CSFR on IFX at 52 weeks. We did not detect any significant associations between gene expression and this outcome, potentially due to the low patient numbers.

Table 1. Demographic and clinical characteristics of study population by subgroups.

	n	Full PROTECT cohort	Gene expression array [GEA]									
			n	Complete GEA cohort	n	Analysed GEA cohort	n	Mesalamine only	n	Moderate-to-severe disease	n	Controls
Demographic												
Age, years	428	12.7 ± 3.3	313	12.9 ± 3.2	284	12.8 ± 3.1	88	12.9 ± 3.1	169	12.9 ± 3.1	20	13.8 ± 3.5
Sex	428		313		284		88		169		20	
Female		212 [50]		147 [47]		132 [46]		43 [49]		76 [45]		11 [55]
Male		216 [50]		166 [53]		152 [54]		45 [51]		93 [55]		9 [45]
Race	420		307		278		86		165		20	
White		351 [84]		259 [84]		237 [85]		69 [80]		144 [87]		17 [85]
Non-white		69 [16]		48 [16]		41 [15]		17 [20]		21 [13]		3 [15]
Ethnicity	424		310		283		87		169		20	
Hispanic or Latino		38 [9]		27 [9]		24 [8]		11 [13]		10 [6]		0
Not Hispanic or Latino		386 [91]		283 [91]		259 [92]		76 [87]		159 [94]		20 [100]
BMI Z score	428	-0.2 ± 1.3	313	-0.2 ± 1.3	284	-0.2 ± 1.3	88	-0.1 ± 1.2	169	-0.3 ± 1.4	20	0.2 ± 1.6
Initial treatment	428		313		284		88		169		20	
Mesalamine		136 [32]		101 [32]		88 [31]		88 [100]		0		0
Oral CS		144 [34]		106 [34]		97 [34]		0		70 [41]		70 [41]
IV CS		148 [35]		106 [34]		99 [35]		0		99 [59]		99 [59]
Clinical												
Disease extent	428		313		284		88		169		20	
Proctosigmoiditis		29 [7]		21 [7]		18 [6]		16 [18]		2 [1]		2 [1]
Left-sided colitis		44 [10]		35 [11]		30 [11]		20 [23]		5 [3]		5 [3]
Extensive/pancolitis		355 [83]		257 [82]		236 [83]		52 [59]		162 [96]		162 [96]
PUCAI score [0–89]	428	50 ± 20	313	50 ± 20	284	51 ± 20	88	31 ± 12	169	64 ± 13	20	13.8 ± 3.5
<45		156 [36]		116 [37]		102 [36]		70 [80]		5 [3]		5 [3]
≥45		272 [64]		197 [63]		182 [64]		18 [20]		164 [97]		164 [97]
Mayo endoscopy sub-score [range 0–]	428	2.2 ± 0.7	313	2.2 ± 0.7	284	2.2 ± 0.7	88	1.8 ± 0.6	169	2.4 ± 0.6	20	13.8 ± 3.5
1 = Mild		59 [14]		45 [14]		39 [14]		28 [32]		6 [3]		6 [3]
2 = Moderate		224 [52]		163 [52]		145 [51]		48 [54]		81 [48]		81 [48]
3 = Severe		145 [34]		105 [34]		100 [35]		12 [14]		82 [49]		82 [49]
Hgb, g/dL	402		294		268		80		162		20	
Mean		11.4 ± 2.2		11.5 ± 2.2		11.5 ± 2.2		12.4 ± 1.8		11 ± 2.2		11 ± 2.2
<10		98 [24]		64 [22]		62 [23]		6 [8]		52 [32]		52 [32]

Table 1. Continued

	n	Full PROTECT cohort	Gene expression array [GEA]					Moderate-to-severe disease	n	Controls
			n	Complete GEA cohort	n	Analysed GEA cohort	n			
CRP	315		313	284	88	169	20			
>ULN	144 [46]		112 [47]		59	140		82 [59]		
>2x ULN	97 [31]		79 [33]		73 [33]	60 [43]		60 [43]		
ESR, mm/h	385		285	258	77	158		30 [17-46]		
Median	2.5 [12-42]		24 [12-39]		24 [12-39]	14 [7-23]		30 [17-46]		
Albumin, g/dL	422		311	282	87	168		3.5 ± 0.7		
Mean	3.7 ± 0.7		3.7 ± 0.7		3.7 ± 0.7	4.0 ± 0.7		69 [41]		
<3.5	138 [33]		100 [32]		92 [33]	13 [15]		28 [23-34]		
Vit D, ng/mL	393		296	268	85	158		21 [13]		
Median	29 [24-35]		28 [24-34]		28 [24-34]	28 [24-34]		71 [45]		
<20	42 [11]		34 [11]		32 [12]	10 [12]		66 [42]		
20-30	183 [46]		140 [47]		127 [47]	44 [52]				
≥30	168 [43]		122 [41]		109 [41]	31 [36]				
Baseline faecal calprotectin, -g/g	239		181	165	49	101				
Median	2352 [1202-3928]		2634 [1212-4022]		2480 [1212-4022]	1629 [772-3632]		3333 [1421-4384]		
>250	226 [95]		171 [94]		155 [94]	40 [82]		100 [99]		
Rectal eosinophils, >32/hpf	367		300	272	84	162		80 [49]		
	210 [57]		161 [54]		144 [53]	45 [54]				

Results are expressed as mean ± SD, n [%] or median [interquartile range]. Analysed GEA cohort excludes patients with protocol violations per PROTECT. IFX, infliximab; PUCAL, Pediatric Ulcerative Colitis Activity Index; BMI, body mass index; CS, corticosteroids; IV, intravenous; Hgb, haemoglobin; CRP, C-reactive protein; ULN, upper limit of normal; ESR, erythrocyte sedimentation rate; vit D, vitamin D; hpf, high-power field.

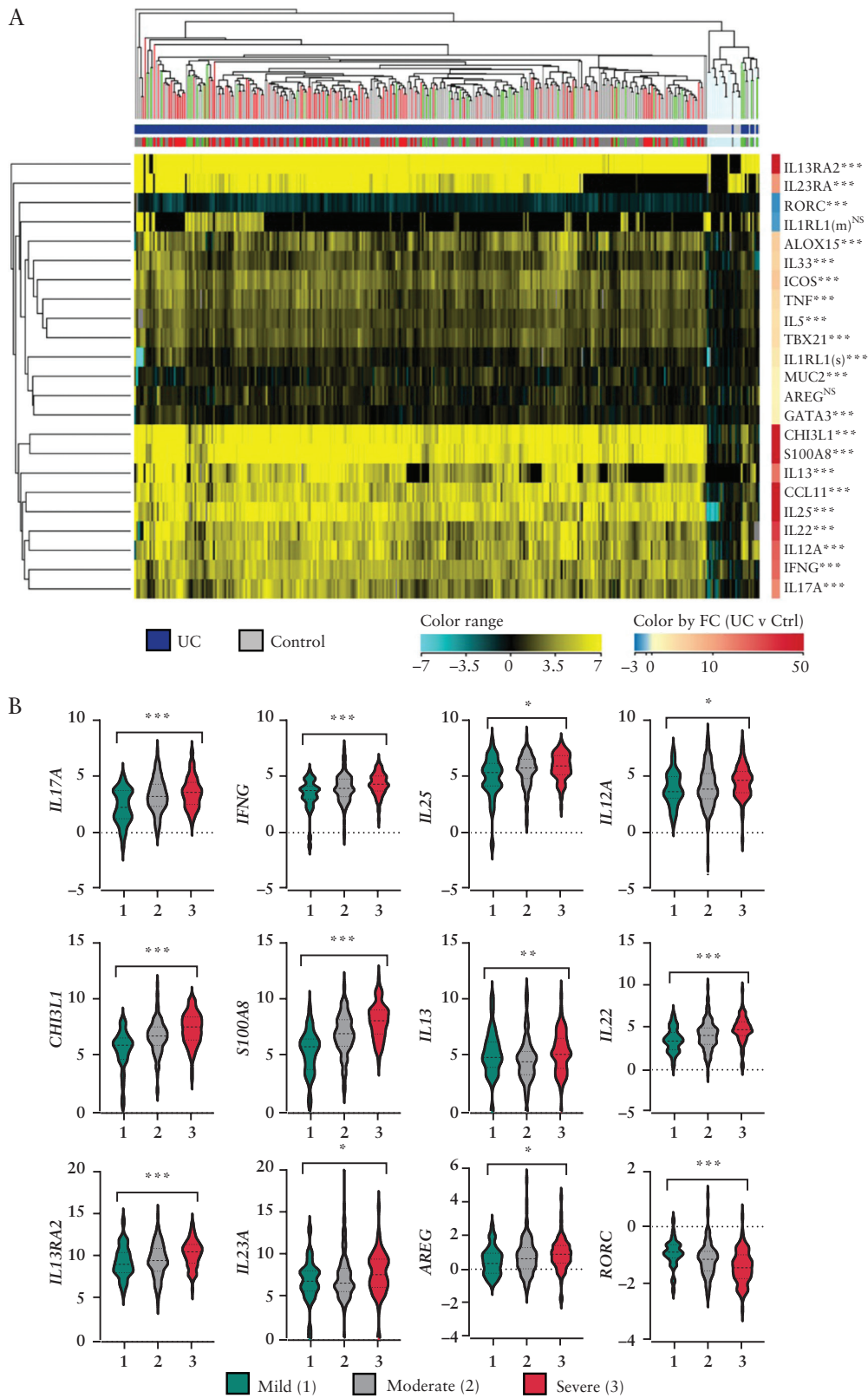


Figure 1. Targeted rectal mucosal gene expression of treatment-naïve paediatric UC patients at diagnosis compared to non-IBD patients. [A] Dendrogram and heatmap of unsupervised hierarchical clustering based on normalized expression of 23 genes as assessed by microfluidic RT-qPCR gene expression array. All *p*-values are false discovery rate-corrected. NS, not significant; **p* < 0.05; ***p* < 0.01; ****p* < 0.001 vs non-IBD controls. [B] Violin plots showing analytes significantly associated with endoscopic Mayo score. The y-axis units are log₂ gene expression relative to controls. **p* < 0.05; ***p* < 0.01; ****p* < 0.001 for Spearman's correlation coefficient across endoscopic Mayo scores 1–3.

Table 2. Significant variables associated with outcomes and predictive models.

Gene expression univariable analysis		Multivariable predictive models								
	OR	<i>p</i> value	OR	<i>p</i> value	AUC	Sen	Spec	LR+	LR-	LR test*
CSFR [week 52]										
<i>IL13RA2</i>	0.83 [0.74–0.94]	0.002	PROTECT Model							
<i>SF00A8</i>	0.84 [0.74–0.96]	0.010	PUCAI < 45	1.87 [1.08–3.24]	0.024	35% [25–45]	86% [81–91]	2.56 [1.61–4.06]	0.76 [0.65–0.88]	NA
<i>RORC</i>	1.49 [0.98–2.28]	0.065	Hgb ≥ 10	3.55 [1.00–12.63]	0.082					
			Wk4 Rem	12.01 [3.51–41.14]	<0.001					
PROTECT Model + <i>IL13RA2</i>										
			PUCAI < 45	1.81 [1.04–3.14]	0.030	45% [35–55]	82% [76–87]	2.48 [1.69–3.64]	0.67 [0.56–0.81]	0.052
			Hgb ≥ 10	3.48 [0.98–12.45]	0.090					
			Wk4 Rem	11.19 [3.25–38.50]	<0.001					
			<i>IL13RA2</i>	0.89 [0.78–1.00]	0.046					
Model without Wk4 data										
			PUCAI < 45	2.20 [1.25–3.87]	0.006	33% [23–43]	89% [83–93]	2.95 [1.74–5.00]	0.76 [0.65–0.88]	0.029
			Hgb ≥ 10	2.28 [1.10–4.74]	0.026					
			Vit D level	1.05 [1.01–1.09]	0.010					
			<i>IL13RA2</i>	0.87 [0.76–0.99]	0.032					
CSNR [week 12]										
<i>IL13</i>	1.28 [1.06–1.54]	0.009	<i>IL13</i>	1.28 [1.06–1.54]	0.009	67% [51–80]	65% [50–79]	1.92 [1.22–3.01]	0.51 [0.32–0.82]	NA
<i>ALOX15</i>	1.38 [0.99–1.92]	0.059								
Escalation to IFX [week 52]										
<i>IL25</i>	1.39 [1.06–1.82]	0.016	<i>IL33</i>	0.66 [0.47–0.93]	0.017	41% [29–53]	74% [64–83]	1.58 [1.02–2.47]	0.80 [0.64–1.00]	NA
<i>IL13RA2</i>	1.25 [1.04–1.50]	0.016	<i>IL13RA2</i>	1.28 [1.06–1.54]	0.010					
<i>IL33</i>	0.68 [0.49–0.94]	0.020								
<i>ALOX15</i>	0.77 [0.61–0.99]	0.040								
Colectomy [week 52]										
<i>RORC</i>	0.28 [0.10–0.78]	0.015	<i>RORC</i>	0.36 [0.14–0.95]	0.040	22% [6–46]	92% [86–96]	2.63 [0.94–7.34]	0.86 [0.68–1.09]	0.033
<i>ALOX15</i>	0.70 [0.48–1.01]	0.056	PUCAI < 45	0.14 [0.02–0.97]	0.050					

95% confidence intervals of predictive statistics are presented in parentheses. Probability cutoffs: 0.5 [CSFR, CSNR, Escalation to IFX]; 0.2 [Colectomy]. CSFR, corticosteroid-free remission; CSNR, corticosteroid-naïve remission; IFX, infliximab; OR, odds ratio; PUCAI, Pediatric Ulcerative Colitis Activity Index; Hgb, haemoglobin; Wk4 Rem, week 4 remission; OR, odds ratio; AUC, area under the curve; Sen, sensitivity; Spec, specificity; LR, likelihood-ratio; NA, not applicable.
*LR test compares the indicated model to the same model including only clinical variables without rectal mucosal gene expression data.

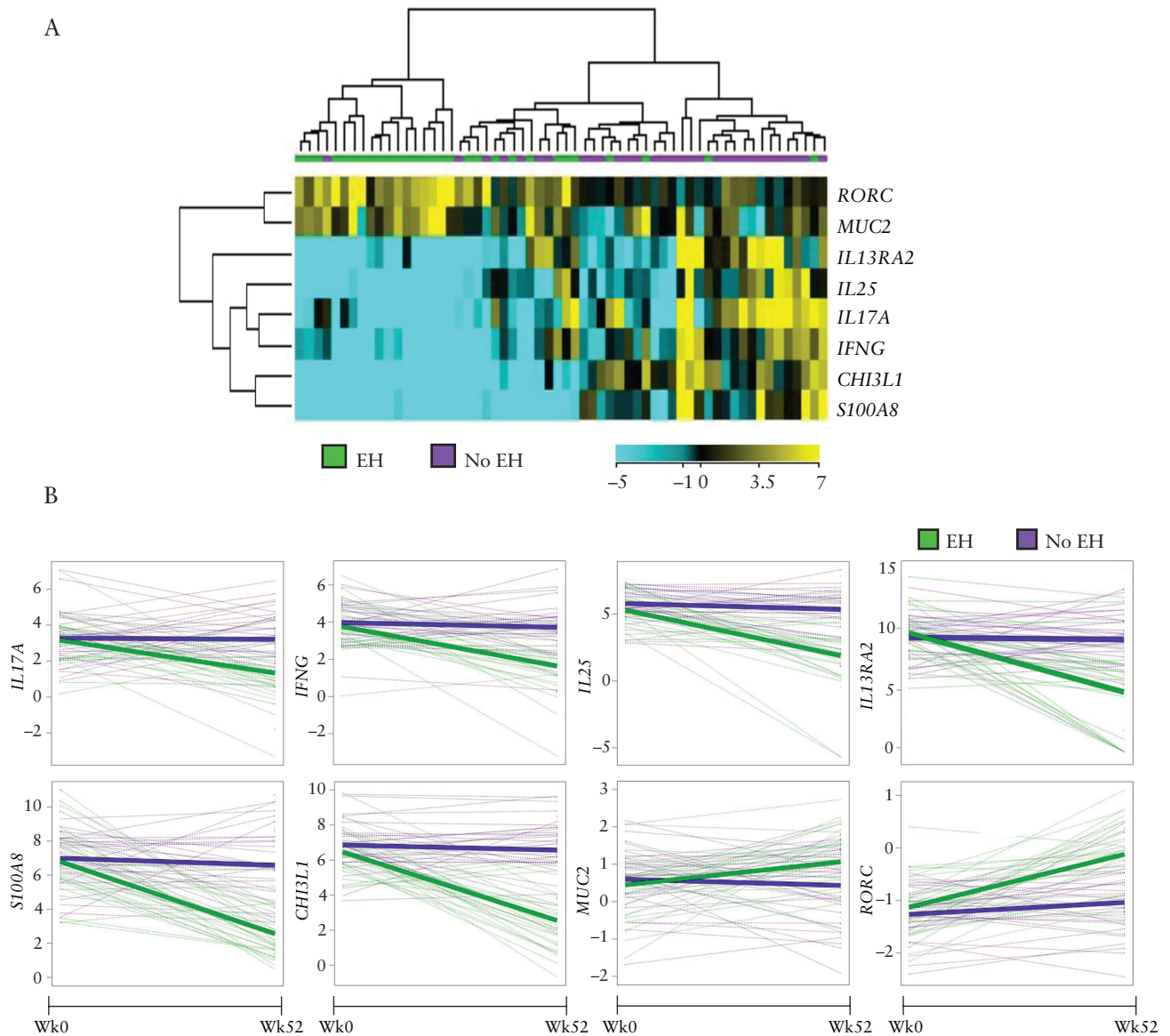


Figure 2. Change in targeted rectal mucosal gene expression from paediatric UC patients between diagnosis and week 52. [A] Dendrogram and heatmap denoting significantly altered gene expression between week 0 and week 52 as assessed by microfluidic RT-qPCR gene expression array for study patients ($n = 58$) with endoscopic healing [EH, endoscopic Mayo score 0] compared to not healed [no EH, endoscopic Mayo score 1–3]. [B] Spaghetti plots with overlying growth curves showing differential change in gene expression from week 0 to week 52 between those with and without endoscopic healing at week 52. The y-axis units are \log_2 gene expression relative to non-IBD control patients.

3.6. RORC expression predicts colectomy by week 52

Nineteen [11%] of the 169 patients with moderate-to-severe disease activity at baseline underwent colectomy by week 52. Univariable logistic regression revealed that increased expression of *RORC* was associated with a lower likelihood of colectomy. There was a trend toward an association of higher *ALOX15* expression with reduced risk for colectomy. A multivariable model including *RORC* and PUCAI predicted risk for colectomy with an AUC of 0.71 [Table 2]. A model including PUCAI alone was inferior to a model including both PUCAI and *RORC* [$p = 0.033$].

3.7. Changes in rectal mucosal gene expression are associated with endoscopic healing

Twelve of the 24 genes correlated with baseline endoscopic Mayo score. Most of the analytes were positively correlated, except *RORC*, which was inversely correlated [Figure 1B].

Twenty-eight [48%] of the 58 patients with 52-week follow-up rectal biopsies achieved endoscopic healing. Baseline characteristics of the patients who underwent follow-up endoscopy were similar to those of the entire cohort [Supplementary Table 2]. No analytes predicted endoscopic healing at 52 weeks for this smaller subset of patients. To determine if endoscopic healing is associated with dynamic changes in gene expression, we compared changes in gene expression from baseline to 52 weeks between patients with and without endoscopic healing. Increasing expression of *RORC* and *MUC2*, and decreasing expression of *IL13RA2*, *IL25*, *IL17A*, *IFNG*, *CHI3L1* and *S100A8* from week 0 to week 52 were associated with endoscopic healing [Figure 2].

3.8. Rectal mucosal expression of type 2 genes is associated with mucosal eosinophils

Eosinophils are recruited or activated by type 2 cytokines.^{6,7} Published analyses from the PROTECT study have

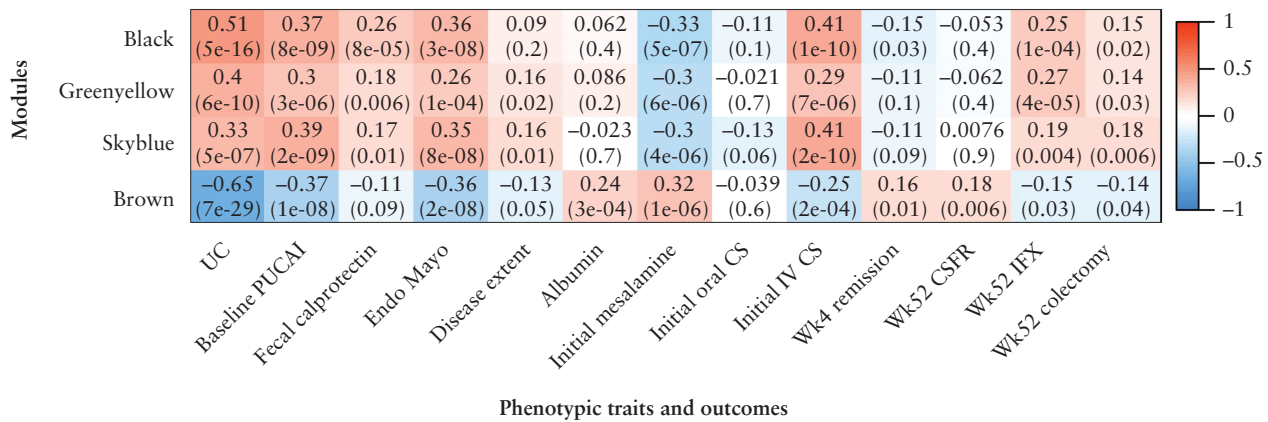


Figure 3. Association of PROTECT RNA-seq gene co-expression modules with phenotypic traits and clinical outcomes. Heatmap of the correlation of selected modules derived from weighted gene co-expression network analysis [WGCNA] of PROTECT RNA-seq data with phenotypic traits and clinical outcomes. The black module contains *IL13RA2*, and the brown module contains *RORC*. *p*-values are shown in parentheses beneath the corresponding Pearson correlation coefficient in each box. UC, ulcerative colitis; PUCAI, Pediatric Ulcerative Colitis Activity Index; Endo, endoscopic; CS, corticosteroids; Wk, week; CSFR, corticosteroid-free remission; IFX, infliximab.

demonstrated that a rectal biopsy eosinophil count of ≤ 32 eosinophils per high-power field [hpf] is associated with treatment escalation or colectomy by 12 weeks in those treated with intravenous corticosteroids and escalation to IFX by 52 weeks in patients with moderate-to-severe disease.^{5,10} We found *ALOX15* [lipoxygenase expressed by eosinophils] and *CCL11* [eosinophil-specific chemokine] expression were significantly associated with a higher rectal eosinophil count, and *IL13* and *IL33* trended toward significance [Supplementary Table 5].

3.9. *IL13RA2* and *RORC* are hubs within UC-associated gene co-expression modules

To further examine the putative roles of *IL13RA2* and *RORC* in paediatric UC, we applied WGCNA to bulk RNA-seq data from the PROTECT study [$n = 206$ UC and $n = 20$ controls]¹¹ to determine whether these outcome-associated genes were contained within disease-relevant gene networks. We identified 16 distinct gene co-expression modules [named with unique colours] significantly correlated with UC. A heatmap of selected modules along with their trait correlations is shown in Figure 3, and a complete heatmap including all module-trait correlations is shown in Supplementary Figure 2.

IL13RA2 was a hub gene, based on both connectivity and phenotype significance scores, within the black module, which positively correlated with measures of disease severity and poor outcomes [escalation to IFX, colectomy; Figure 3]. *IL13RA2* co-expressed genes within the black module were associated with extracellular matrix, collagen binding, cytokine activity, inflammatory response and abnormal innate immunity [Figure 4A].

RORC was a hub gene within the brown module. Similar to *RORC* gene expression alone, the brown module negatively correlated with disease severity and poorer outcomes [escalation to IFX, colectomy] and positively correlated with superior outcomes [week 4 remission and CSFR at 52 weeks]. *RORC* co-expressed genes within the brown module were involved in lipid binding, lipid metabolic processes, steroid hormone receptor activity and microvillous assembly [Figure 4B].

Two additional modules, greenyellow and skyblue, showed strong positive correlations with disease severity and poorer

outcomes. The greenyellow module was associated with host entry and immune response, and the skyblue module was associated with cytokine production and leukocyte chemotaxis [Supplementary Figure 3].

3.10. Single-cell RNA-seq reveals cell-specific dysregulation of *RORC* and *IL13RA2* in adult UC

To gain an understanding of the cellular sources of *RORC* and *IL13RA2* and their associated gene expression modules in UC, we analysed a publicly available adult colon single-cell RNA-seq data set including inflamed and non-inflamed UC tissues, and tissues from non-IBD controls.¹⁶ That study previously described that *IL13RA2* expression marked a distinct subset of inflammatory fibroblasts associated with UC. Accordingly, we found that expression of *IL13RA2* and its 20 most highly correlated genes within the black module were expressed in inflammatory fibroblasts [Figure 5A].

RORC encodes the nuclear receptor $ROR\gamma$, including its isoform $ROR\gamma T$, the canonical type 17 transcription factor. Given that expression of other type 17 genes [*IL17*, *IL23*] were increased in UC [Figure 1], but *RORC* and its brown module were associated with healthy colon and superior outcomes, we questioned whether disease-associated alterations in *RORC* were immune cell-intrinsic. Analysis of this single-cell RNA-seq data set showed that *RORC* and its brown module-correlated genes are expressed in colon epithelial cells, specifically stem cells and transit amplifying [TA] cells [Figure 5A].

We then examined disease-state differential expression of *IL13RA2* and *RORC* in this data set. As expected, *IL13RA2* was expressed in inflammatory fibroblasts from inflamed and non-inflamed UC tissues, but not non-IBD tissues [Supplementary Figure 4A]. *RORC* was detected in ~20% of epithelial stem cell and TA cell subsets [Figure 5A and Supplementary Figure 4B]. This may be related to stochastic detection of expression for low- to moderately expressed genes by single-cell RNA-seq pipelines.²¹ Therefore, we compared normalized *RORC* expression within epithelial stem cells, secretory TA cells, TA2 cells and cycling TA cells with detectable *RORC* expression between disease states. We observed reduced *RORC* expression in *RORC*-expressing stem

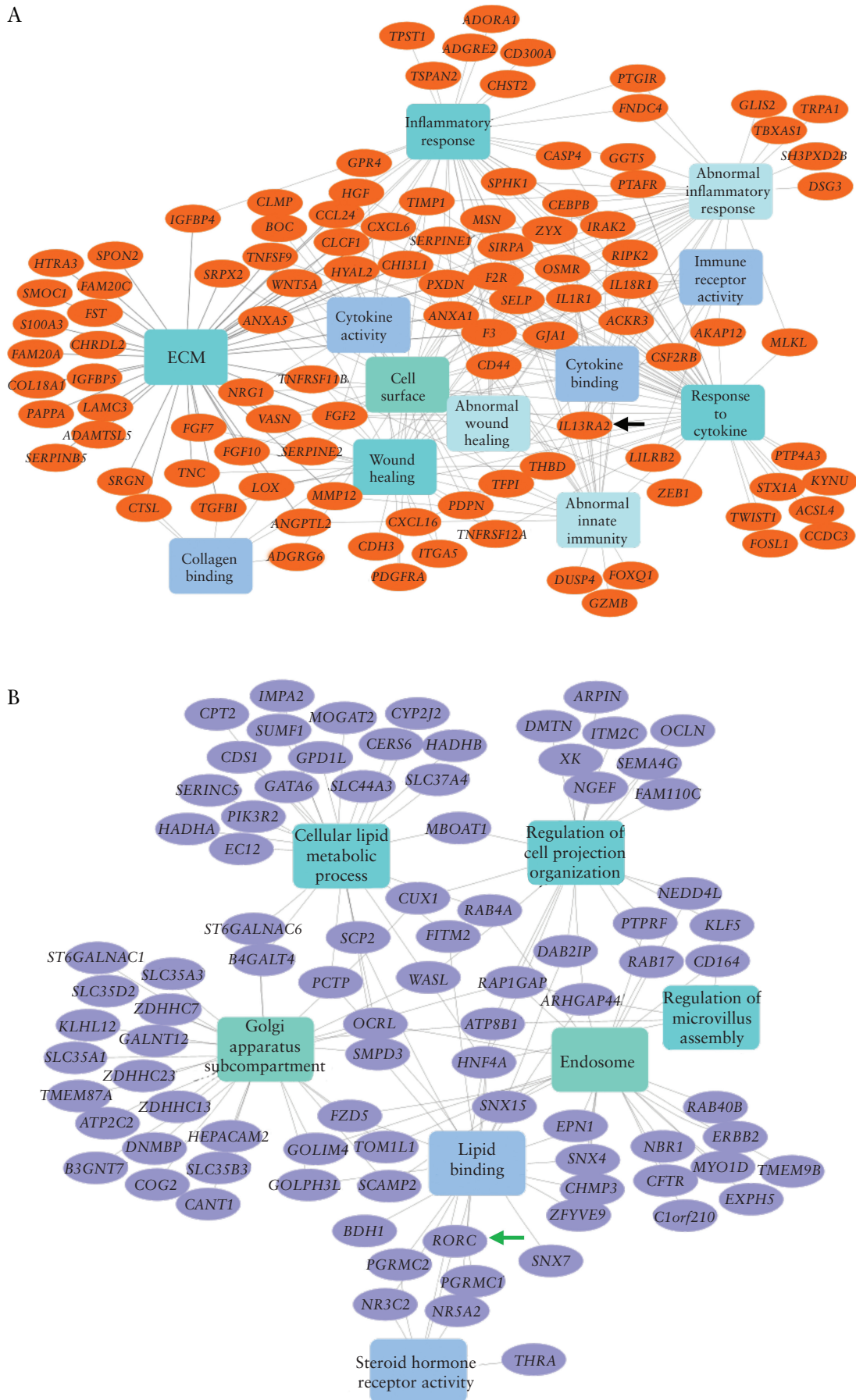


Figure 4. Network representation of significantly enriched terms [rectangles] of *IL13RA2* and *RORC* top-correlated genes [ovals] from the black and brown modules, respectively. [A] Black module containing *IL13RA2*, indicated by the black arrow. [B] Brown module containing *RORC*, indicated by the green arrow.

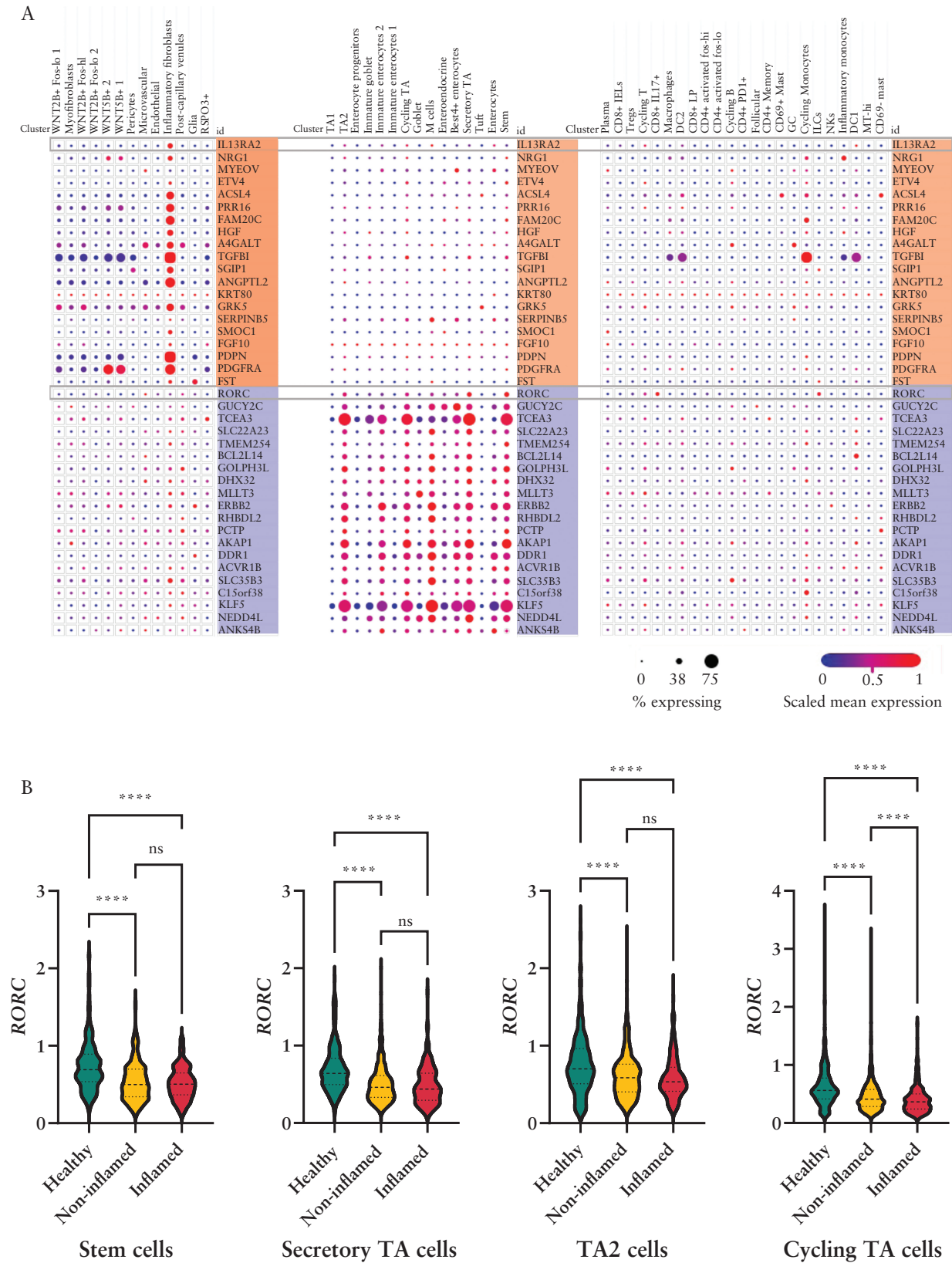


Figure 5. Cell-specific expression of *IL13RA2* and *RORC* and their most closely correlated genes. [A] Expression of *IL13RA2* and its 20 most closely correlated genes within the black module [shaded in orange] and *RORC* and its 20 most closely correlated genes from the brown module [shaded in purple] within stromal, epithelial and immune cell types from existing adult colon UC single-cell RNA-seq data.¹⁶ The size and colour of the dots are proportional to the percentage expressing the gene and the normalized expression level, respectively. [B] Further analysis of the same adult single-cell RNA-seq data set comparing *RORC* expression within non-zero expressing cells between healthy, non-inflamed UC, and inflamed UC from specific epithelial cell types. The y-axis units for *RORC* expression are $\log_2[\text{TP10K} + 1]$. NS, not significant; **** $p < 0.0001$. TA, transit amplifying.

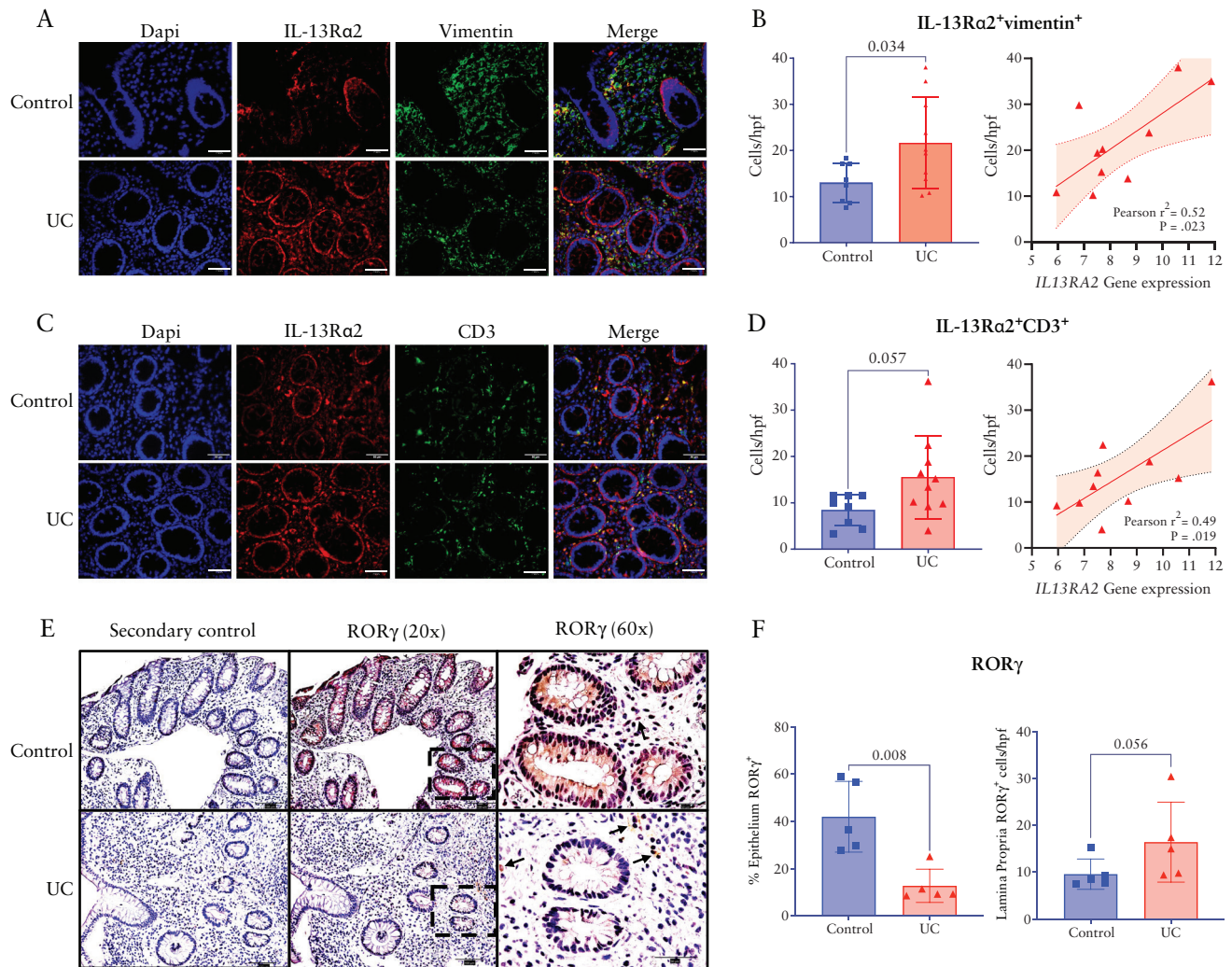


Figure 6. IL-13Rα2 and RORγ protein localization in paediatric UC tissues. Representative immunofluorescence images showing IL-13Rα2 co-localization with vimentin [A] and CD3 [C]; 40× magnification [scale bars = 50 μm]. Comparison of the number of IL-13Rα2+vimentin+ [B] or IL-13Rα2+CD3+ cells [D] per high-power field between UC and non-IBD control patients and correlation with *IL13RA2* gene expression within UC tissues. Representative images of immunohistochemical staining for RORγ protein expression [brown] in UC and non-IBD control tissues at 20× [scale bars = 100 μm] and 60× magnification [scale bars = 50 μm]. Images from staining with secondary antibody are displayed as a negative control. Location of the 60× high-power image is indicated by the dashed bordered box overlying the 20× magnification image. Arrows indicate RORγ+ lamina propria cells. Comparison of the percentage of the epithelium positively stained for RORγ and the number of RORγ+ lamina propria cells/hpf between non-IBD control and UC tissues [F]. hpf, high power field; UC, ulcerative colitis.

cells, secretory TA cells, TA2 cells and cycling TA cells from inflamed and non-inflamed UC tissues compared to non-IBD tissues [Figure 5B]. These observations further support that the reduced tissue expression of RORC in UC is derived from reduced expression in epithelial stem and TA cells.

We performed immunofluorescence staining and immunohistochemistry to localize IL-13Rα2 and RORγ protein expression, respectively. Previous reports have localized IL-13Rα2 to fibroblasts or T cells.^{16,22,23} There were significantly more IL-13Rα2+vimentin+ fibroblasts populating the colon lamina propria in paediatric UC compared to non-IBD controls [$p = 0.034$, Figure 6A and 6B]. There was also a trend toward an increase in IL-13Rα2+CD3+ T cells in UC compared to non-IBD [$p = 0.057$, Figure 6C and 6D]. IL-13Rα2 was ubiquitously expressed in epithelial cells of both UC and non-IBD controls. Numbers of both IL-13Rα2+vimentin+ fibroblasts and IL-13Rα2+CD3+ T cells correlated with *IL13RA2* gene expression in paediatric UC [Figure 6B and 6D]. Consistent with the bulk and single-cell

RNA-seq analyses, the epithelium of UC tissues exhibited significantly less expression of RORγ compared to that of non-IBD control tissue [$p = 0.008$]. Also, consistent with our finding of increased *IL17A* expression in UC, there was a trend toward increased numbers of RORγ+ cells populating the lamina propria of UC tissues compared to that of non-IBD control tissues [$p = 0.056$; Figure 6E and 6F].

4. Discussion

In a well-established cohort of treatment-naïve paediatric UC patients treated with standardized mesalamine and CS, we show that targeted assessment of baseline rectal mucosal immune gene expression predicts clinical outcomes. A model including *IL13RA2* and only baseline clinical parameters was as accurate for predicting CSFR as an established clinical model that requires week 4 remission status. Furthermore, our findings validate the association of type 2 immune genes [*IL13*, *IL33*] with positive outcomes, and *IL13RA2*, which

decreases the bioactivity of IL-13 [a key effector type 2 cytokine], with poorer outcomes, suggesting a protective role of type 2 cytokines in UC. We observed signals of *IL13RA2* expression associated with poor outcomes and *RORC* with superior outcomes. Our analysis of publicly available bulk and single-cell data sets support that *IL13RA2* is a hub gene within an inflammatory fibroblast gene co-expression module upregulated in UC associated with extracellular matrix and innate immune response. We found *RORC* to be a hub gene within an epithelial stem and TA cell co-expression module associated with lipid binding and metabolism, steroid hormone receptor activity, and microvillus assembly.

Studies of cytokine secretion from lamina propria immune cells of adult UC surgical tissues established the association of a type 2 immune response with UC.^{7,24} Our group has now demonstrated upregulation of *IL13* expression in two treatment-naïve paediatric UC cohorts, and previously showed this was specific to paediatric UC over Crohn's colitis.⁸ Previous studies have supported that IL-13 is produced by atypical natural killer T cells bearing IL-13R α 2 that exert epithelial cytotoxicity and are pathogenic in UC.^{22,25} However, there is an emerging understanding of the protective roles of type 2 immune responses in UC related to promotion of tissue repair and differentiation of mucin-secreting goblet cells.^{6,26} The negative results of clinical trials of two anti-IL-13 monoclonal antibodies for the treatment of UC contradicts the theory of a primary pathogenic role for IL-13.^{27,28} In fact, in a smaller treatment-naïve paediatric UC cohort treated with standard care, our group found that a tissue gene expression pattern marked by detectable expression of *IL13* was associated with improved clinical outcomes.⁸ Here, in a larger independent treatment-naïve cohort in which we examined specific treatment pathways, we validate our previous findings with the observation that *IL13* expression is associated with CSNR at 12 weeks in patients treated with mesalamine alone at diagnosis. Interestingly, amongst paediatric patients with baseline moderate-to-severe UC, expression of the type 2 instructive cytokine *IL33* was also associated with a lower likelihood of escalation to IFX. Collectively, these findings support that a type 2 immune response in UC may be a protective response to inflammation that improves treatment outcomes.

We observed that increased baseline rectal mucosal *IL13RA2* expression was associated with a lower likelihood of CSFR, higher likelihood of escalating to IFX therapy by 1 year and higher baseline endoscopic severity. *IL13RA2* expression was associated with increased disease severity as evidenced by correlations with endoscopic Mayo score and *S100A8* expression. Nonetheless, it informed our predictive models better than baseline faecal calprotectin [which had no detectable association with clinical outcomes] and histological severity score. Several lines of evidence implicate *IL13RA2* in the pathogenesis of IBD. *IL13RA2* encodes an alternative receptor for IL-13 [classically described as a decoy receptor] with both membrane-bound and soluble forms that block the activity of IL-13.²⁹ However, some have reported IL-13R α 2 signalling activity.³⁰ Mucosal expression of *IL13RA2* is associated with resistance to anti-TNF therapy in both adult UC and Crohn's disease.^{31,32} Single-cell RNA-seq has revealed enrichment of inflammatory fibroblasts expressing *IL13RA2* in adult UC that are similarly associated with anti-TNF resistance.¹⁶ Receptor–ligand analysis proposed a strong interaction between inflammatory monocytes and

IL13RA2⁺*IL11*⁺ inflammatory fibroblasts expressing the receptor for oncostatin M, another monocyte-derived cytokine implicated in treatment resistance.^{11,33,34} It is suspected that *IL13RA2* negatively regulates IL-13 signalling and blocks its anti-inflammatory effects, supported by the observation that *IL13RA2* knockout mice exhibit increased IL-13 activity and are protected against both acute and chronic models of colitis.^{20,35,36} Interestingly, *IL13RA2* was not within the published PROTECT antimicrobial RNA-seq gene expression signature that strengthened the predictive models for CSFR and escalation to IFX therapy.⁵ Here, we may have been better poised to detect the association of *IL13RA2* with poor outcomes due to our use of different technology [RT-qPCR microfluidic array] or the stringent multiple comparison correction required for higher order transcriptomic data analysed in PROTECT. Consistent with a role for *IL13RA2* in inflammatory fibroblasts and monocyte interactions, we found that in UC patients, *IL13RA2* was a hub gene with *OSMR* within a co-expression module associated with extracellular matrix, cytokine activity and innate immune response. As a whole, our findings corroborate adult IBD studies by demonstrating the utility of mucosal *IL13RA2* for improving outcome prediction in paediatric UC over clinical models alone and provide further evidence that the role of *IL13RA2* in UC pathogenesis involves expression by inflammatory fibroblasts.

RORC encodes the nuclear receptor ROR γ and its isoform ROR γ T, the latter being the canonical Th17 transcription factor. Higher baseline *RORC* expression is associated with improved response to anti-TNF therapy and endoscopic healing in adult UC patients.³⁷ One would expect *RORC* to be upregulated in UC compared to healthy controls given the upregulation of type 17 instructive and effector cytokines we observed. However, we found that *RORC* was net downregulated in UC and inversely associated with endoscopic severity. Furthermore, we observed that increased *RORC* expression was associated with improved outcomes, including a lower likelihood of colectomy at 1 year. In line with our findings, an independent analysis of PROTECT bulk RNA-seq data found *RORC* to be one of nine genes within a transcriptional risk score, derived from differential expression of UC risk genes that are also expression quantitative trait loci [eQTL], predictive of colectomy at 52 weeks.³⁸ Our WGCNA of RNA-seq PROTECT data mirrored these findings, as the module containing *RORC* was associated with lower severity and positive outcomes. Interestingly, our functional enrichment analysis suggests that *RORC* is involved in epithelial cell lipid metabolic and structural processes rather than primarily immune cells. *RORC* and its co-expressed genes within this module mapped to epithelial stem cells and less-differentiated transit-amplifying cells in an adult UC single-cell RNA-seq data set. This observation is in line with a previous report of *RORC* expression in the colon epithelium at crypt bases in human colon and mouse models.³⁹ Our analysis of published single-cell RNA-seq data and tissue immunostaining confirmed epithelial downregulation of ROR γ protein in UC. Regarding other organ systems, there have been reports of ROR γ expression localizing to epithelial cells in skin,⁴⁰ and of ROR γ mediating the epithelial–mesenchymal transition in breast cancer and hepatic fibrosis.^{41,42} One interesting hypothesis deserving of further study is that colon epithelial-intrinsic ROR γ may have a role in epithelial wound repair.

A notable strength of our study was use of the large PROTECT inception cohort, free from confounding by

previous therapy. Other strengths include the analysis of 52-week follow-up rectal biopsies, and confirmation of findings through RNA-seq WGCNA and single-cell analysis. We were able to validate our previously published association of *IL13* expression with positive outcomes in this larger cohort and narrow its predictive capacity to mesalamine response. Limitations of our study include measuring mRNA gene expression rather than protein analysis, though previous studies have shown sufficient correlation between cytokine gene expression measured by real-time RT-qPCR and protein abundance.⁴³ In addition, there is no comparable paediatric UC cohort for validation of new signals identified. This weakness is mitigated by our approach to examine signals through targeted GEA and RNA-seq, and by the observation that *IL13RA2* has previously been associated with poor response to therapy in adults.^{31,44} Although, at the cut-off values chosen, our models exhibit low sensitivity, specificities were fairly high. Cut-off values were based on pre-selected probabilities and could be modified to favour sensitivity or specificity. For instance, specificity for the model for colectomy was quite high, and therefore a positive test may accurately identify patients at very high risk for colectomy who may benefit from early treatment with anti-TNF therapy.

In conclusion, in a large treatment-naïve paediatric UC inception cohort, targeted assessment of mucosal immune gene expression predicted clinical outcomes. A model including baseline gene expression and clinical factors was as accurate for predicting CSFR as an established clinical model, which requires week 4 remission status. Association of type 2 immune genes with improved outcomes, and the type 2 counteracting gene *IL13RA2* with poorer outcomes, implies a beneficial role of type 2 cytokines in UC. Our findings support those of others associating *IL13RA2* from inflammatory fibroblasts with the innate immune response and extracellular matrix functions and poor response to therapy. Increased expression of *RORC*, probably from crypt base stem and TA cells, is associated with lipid metabolism and cell structure and a lower likelihood of colectomy. These findings support further exploration of IL-13R α 2 as a therapeutic target in UC and future studies of the epithelial-specific role of *RORC* in colon mucosal homeostasis and UC pathogenesis.

Funding

This work was supported by the National Institute of Diabetes and Digestive and Kidney Diseases of the National Institutes of Health [R01DK117119 to M.J.R., U01DK095745 to J.S.H. and L.A.D., and T32DK007727 to K.C.]. This project was also supported in part by NIH P30 DK078392 Gene Analysis and Clinical Component Scores of the Digestive Diseases Research Core Center in Cincinnati, OH. Data management was further supported by the Center for Clinical and Translational Science and Training funded in part by the National Center for Advancing Translational Sciences [2UL1TR001425].

Conflict of Interest

MJR has served on an advisory board for Entasis Therapeutics. JSH has served on advisory boards for Janssen and AbbVie, and as a consultant for Pfizer, Lilly, Takeda, BMS and Thetis Pharmaceuticals. JRR has served on an advisory board for BMS and Lilly and has received grant/research support

from AbbVie and Janssen. ASP has served as a consultant for AbbVie. NSL has served on a data monitoring board for AbbVie. TDW has served as a consultant for Janssen Canada, AbbVie Canada and Merck Canada. All other authors declare no competing interests.

Author Contributions

Conceptualization: MJR, LAD, RK, JSH, YH. Data curation: TDW, RK, KC, MJR. Formal analysis: KC, RK, AGJ, MS, YH. Funding acquisition: MJR, LAD, JSH. Investigation: KC, MJR, SF, BAO, PM, TDW, AMG, DRM, BB, NSL, JM, JRR, ASP, SS, RNB, MP, CS, SK, JSH, LAD. Methodology: RK, AGJ. Project administration: MJR, KC. Resources/provision of patient samples: PM, TDW, AMG, DRM, BB, NSL, JM, JRR, ASP, SS, RNB, MP, CS, SK, JSH, LAD, MJR. Supervision: MJR. Visualization: KC, RK, SF, BAO, AGJ, MS. Drafting of manuscript: KC, SF, BAO. Critical review and editing of manuscript: PM, TDM, AMG, DRM, BB, NSL, JM, JRR, ASP, SS, RNB, MP, CS, SK, YH, JSH, LAD, MJR.

Data Availability

Statement: Data from the PROTECT study will be available from the US National Institutes of Diabetes, and Digestive and Kidney Diseases data repository [<https://repository.niddk.nih.gov/home/>]. Requestors can apply for access via this website and must have approval from their institution's review board.

Supplementary Data

Supplementary data are available online at *ECCO-JCC* online.

References

- Ye Y, Manne S, Treem WR, *et al.* Prevalence of inflammatory bowel disease in pediatric and adult populations: recent estimates from large national databases in the United States, 2007–2016. *Inflamm Bowel Dis* 2020;**26**:619–25.
- Roberts SE, Thorne K, Thapar N, *et al.* A systematic review and meta-analysis of paediatric inflammatory bowel disease incidence and prevalence across Europe. *J Crohns Colitis* 2020;**14**:1119–48.
- Kaplan GG, Ng SC. Understanding and preventing the global increase of inflammatory bowel disease. *Gastroenterology* 2017;**152**:313–321.e2.
- Sykora J, Pomahacova R, Kreslova M, *et al.* Current global trends in the incidence of pediatric-onset inflammatory bowel disease. *World J Gastroenterol* 2018;**24**:2741–63.
- Hyams JS, Davis Thomas S, Gotman N, *et al.* Clinical and biological predictors of response to standardised paediatric colitis therapy (PROTECT): a multicentre inception cohort study. *Lancet* 2019;**393**:1708–20.
- Wynn TA. Type 2 cytokines: mechanisms and therapeutic strategies. *Nat Rev Immunol* 2015;**15**:271–82.
- Fuss IJ, Neurath M, Boirivant M, *et al.* Disparate CD4+ lamina propria (LP) lymphokine secretion profiles in inflammatory bowel disease. Crohn's disease LP cells manifest increased secretion of IFN-gamma, whereas ulcerative colitis LP cells manifest increased secretion of IL-5. *J Immunol* 1996;**157**:1261–70.
- Rosen MJ, Karns R, Vallance JE, *et al.* Mucosal expression of type 2 and type 17 immune response genes distinguishes ulcerative colitis from colon-only Crohn's disease in treatment-naïve pediatric patients. *Gastroenterology* 2017;**152**:1345–1357.e7.
- Sparano JA, Gray RJ, Makower DF, *et al.* Adjuvant chemotherapy guided by a 21-gene expression assay in breast cancer. *N Engl J Med* 2018;**379**:111–21.

10. Hyams JS, Davis S, Mack DR, et al. Factors associated with early outcomes following standardised therapy in children with ulcerative colitis (PROTECT): a multicentre inception cohort study. *Lancet Gastroenterol Hepatol* 2017;2:855–68.
11. Haberman Y, Karns R, Dexheimer PJ, et al. Ulcerative colitis mucosal transcriptomes reveal mitochondriopathy and personalized mechanisms underlying disease severity and treatment response. *Nat Commun* 2019;10:38.
12. Haberman Y, Iqbal NT, Ghandikota S, et al. Mucosal genomics implicate lymphocyte activation and lipid metabolism in refractory environmental enteric dysfunction. *Gastroenterology* 2021;160:2055–2071.e0.
13. Zhang B, Horvath S. A general framework for weighted gene co-expression network analysis. *Stat Appl Genet Mol Biol* 2005;4:Article17.
14. Chen J, Bardes EE, Aronow BJ, et al. ToppGene Suite for gene list enrichment analysis and candidate gene prioritization. *Nucleic Acids Res* 2009;37:W305–11.
15. Shannon P, Markiel A, Ozier O, et al. Cytoscape: a software environment for integrated models of biomolecular interaction networks. *Genome Res* 2003;13:2498–504.
16. Smillie CS, Biton M, Ordovas-Montanes J, et al. Intra- and inter-cellular rewiring of the human colon during ulcerative colitis. *Cell* 2019;178:714–730.e22.
17. Crowe AR, Yue W. Semi-quantitative determination of protein expression using immunohistochemistry staining and analysis: an integrated protocol. *Bio Protoc* 2019;9:e3465.
18. Ruifrok AC, Johnston DA. Quantification of histochemical staining by color deconvolution. *Anal Quant Cytol Histol* 2001;23:291–9.
19. Monticelli LA, Sonnenberg GF, Abt MC, et al. Innate lymphoid cells promote lung-tissue homeostasis after infection with influenza virus. *Nat Immunol* 2011;12:1045–54.
20. Karmele EP, Pasricha TS, Ramalingam TR, et al. Anti-IL-13Ralpha2 therapy promotes recovery in a murine model of inflammatory bowel disease. *Mucosal Immunol* 2019;12:1174–86.
21. Kim JK, Kolodziejczyk AA, Ilicic T, et al. Characterizing noise structure in single-cell RNA-seq distinguishes genuine from technical stochastic allelic expression. *Nat Commun* 2015;6:8687.
22. Fuss IJ, Joshi B, Yang Z, et al. IL-13Ralpha2-bearing, type II NKT cells reactive to sulfatide self-antigen populate the mucosa of ulcerative colitis. *Gut* 2014;63:1728–36.
23. Graham DB, Xavier RJ. Pathway paradigms revealed from the genetics of inflammatory bowel disease. *Nature* 2020;578:527–39.
24. Fuss IJ, Heller F, Boirivant M, et al. Nonclassical CD1d-restricted NK T cells that produce IL-13 characterize an atypical Th2 response in ulcerative colitis. *J Clin Invest* 2004;113:1490–7.
25. Heller F, Florian P, Bojarski C, et al. Interleukin-13 is the key effector Th2 cytokine in ulcerative colitis that affects epithelial tight junctions, apoptosis, and cell restitution. *Gastroenterology* 2005;129:550–64.
26. Monticelli LA, Osborne LC, Noti M, et al. IL-33 promotes an innate immune pathway of intestinal tissue protection dependent on amphiregulin-EGFR interactions. *Proc Natl Acad Sci USA* 2015;112:10762–7.
27. Danese S, Rudzinski J, Brandt W, et al. Tralokinumab for moderate-to-severe UC: a randomised, double-blind, placebo-controlled, phase IIa study. *Gut* 2015;64:243–9.
28. Reinisch W, Panes J, Khurana S, et al. Anrukinzumab, an anti-interleukin 13 monoclonal antibody, in active UC: efficacy and safety from a phase IIa randomised multicentre study. *Gut* 2015;64:894–900.
29. Hershey GK. IL-13 receptors and signaling pathways: an evolving web. *J Allergy Clin Immunol* 2003;111:677–90; quiz 691; quiz 691.
30. Fichtner-Feigl S, Strober W, Kawakami K, et al. IL-13 signaling through the IL-13alpha2 receptor is involved in induction of TGF-beta1 production and fibrosis. *Nat Med* 2006;12:99–106.
31. Arijs I, Li K, Toedter G, et al. Mucosal gene signatures to predict response to infliximab in patients with ulcerative colitis. *Gut* 2009;58:1612–9.
32. Verstockt B, Verstockt S, Creyns B, et al. Mucosal IL13RA2 expression predicts nonresponse to anti-TNF therapy in Crohn's disease. *Aliment Pharmacol Ther* 2019;49:572–81.
33. West NR, Hegazy AN, Owens BMJ, et al. Oncostatin M drives intestinal inflammation and predicts response to tumor necrosis factor-neutralizing therapy in patients with inflammatory bowel disease. *Nat Med* 2017;23:579–89.
34. Hyams JS, Brimacombe M, Haberman Y, et al. Clinical and host biological factors predict colectomy risk in children newly diagnosed with ulcerative colitis. *Inflamm Bowel Dis* 2022;28:151–60.
35. Wilson MS, Ramalingam TR, Rivollier A, et al. Colitis and intestinal inflammation in IL10^{-/-} mice results from IL-13Ralpha2-mediated attenuation of IL-13 activity. *Gastroenterology* 2011;140:254–64.
36. Verstockt B, Perrier C, De Hertogh G, et al. Effects of epithelial IL-13Ralpha2 expression in inflammatory bowel disease. *Front Immunol* 2018;9:2983.
37. Viazis N, Giakoumis M, Bamias G, et al. Predictors of tissue healing in ulcerative colitis patients treated with anti-TNF. *Dig Liver Dis* 2017;49:29–33.
38. Mo A, Nagpal S, Gettler K, et al. Stratification of risk of progression to colectomy in ulcerative colitis via measured and predicted gene expression. *Am J Hum Genet* 2021;108:1765–79.
39. Modica S, Gofflot F, Murzilli S, et al. The intestinal nuclear receptor signature with epithelial localization patterns and expression modulation in tumors. *Gastroenterology* 2010;138:636–48, 648.e1, 648 e1-12.
40. Slominski AT, Kim TK, Takeda Y, et al. RORalpha and ROR gamma are expressed in human skin and serve as receptors for endogenously produced noncalcemic 20-hydroxy- and 20,23-dihydroxyvitamin D. *FASEB J* 2014;28:2775–89.
41. Oh TG, Wang SM, Acharya BR, et al. The nuclear receptor, RORgamma, regulates pathways necessary for breast cancer metastasis. *EBioMedicine* 2016;6:59–72.
42. Kim SM, Choi JE, Hur W, et al. RAR-related orphan receptor gamma [ROR-gamma] mediates epithelial–mesenchymal transition of hepatocytes during hepatic fibrosis. *J Cell Biochem* 2017;118:2026–36.
43. Flores MG, Zhang S, Ha A, et al. In vitro evaluation of the effects of candidate immunosuppressive drugs: flow cytometry and quantitative real-time PCR as two independent and correlated read-outs. *J Immunol Methods* 2004;289:123–35.
44. Verstockt B, Perrier C, De Hertogh G, et al. Effects of epithelial IL-13Ralpha2 expression in inflammatory bowel disease. *Front Immunol* 2018;9.